A&A 391, 571–576 (2002)
DOI: 10.1051/0004-6361:20020778

Astronomy & Astrophysics

XMM-Newton observations of the isolated neutron star RX J0806.4-4123 ⋆

F. Haberl and V. E. Zavlin

Max-Planck-Institut für extraterrestrische Physik, Giessenbachstraße, 85748 Garching, Germany

Received 3 April 2002 / Accepted 16 May 2002

Abstract. The isolated neutron star RX J0806.4-4123 was observed with XMM-Newton in November 2000. The data from the three EPIC instruments allowed us (i) to derive an improved X-ray position to an accuracy of 2–3″, (ii) to accumulate the first medium-resolution soft X-ray spectra of high statistical quality and (iii) to find a candidate for the neutron star rotation period. Although this period of 11.3714 s is formally detected at a 3.5σ level in the EPIC-pn data, the similar pulse profiles deduced from all three EPIC instruments increase the confidence that the period is real. The pulsed fraction of ∼6% would then be the weakest X-ray flux modulation detected from dim isolated neutron stars. We fitted the X-ray spectra with blackbody and neutron star atmosphere models and discuss the results with respect to the brightness limit placed by optical images. The reduced size of the error circle on the X-ray position should allow deeper searches for an optical counterpart.

Key words. X-rays: stars – stars: neutron – stars: magnetic fields – stars: individual: RX J0806.4-4123

1. Introduction

The ROSAT all-sky survey source RX J0806.4-4123 (1RXS J080623.0-412233) was suggested as candidate for an isolated neutron star (INS) by Haberl et al. (1998) based on X-ray properties of this source similar to the established cases RX J1856.5-3754 (Walter et al. 1996) and RX J0720.4-3125 (Haberl et al. 1997). While the latter two (the brightest in the sample of INSs discovered with ROSAT) were optically identified with $m_V \sim 25.6$ (Walter & Matthews 1997) and $m_B \sim 26$ (Motch & Haberl 1998; Kulkarni & van Kerkwijk 1998) blue objects, respectively, optical observations of RX J0806.4-4123 were only able to derive a limiting B magnitude $m_B > 24$ for a possible optical counterpart (Haberl et al. 1998). High resolution X-ray spectra obtained from RX J1856.5-3754 and RX J0720.4-3125 have revealed no evidence for photospheric absorption or emission features and are well modeled as blackbody radiation with little interstellar absorption (Paerels et al. 2001; Burwitz et al. 2001).

Today seven ROSAT discovered INSs (hereafter dim INS) are known (see references in Motch 1999; Zampieri et al. 2001) with RX J0720.4-3125 (rotation period $P = 8.39$ s; Haberl et al. 1997), RX J0420.0-5022 ($P = 22.7$ s; Haberl et al. 1999) and RBS 1223 ($P = 5.16$ s; Hambaryan et al. 2002) showing pulsations in the X-ray flux. No radio emission has been detected yet from these objects. While little doubt is left that these objects are indeed INSs, the origin of their X-rays is still a matter of debate. If we see thermal emission from young cooling neutron stars, the observed blackbody temperatures in the range of 50–120 eV imply ages younger than $\sim 10^6$ years for standard cooling curves. Older neutron stars may be re-heated by accretion of interstellar matter, producing X-ray luminosities sufficiently high to be observable. However, the accretion rate strongly depends on the velocity of the neutron star relative to the interstellar medium, and the neutron star must rotate slowly enough to allow the matter to enter the magnetosphere (see the review of Treves et al. 2000). The recent estimates of a pulse period derivative of $(0.7–2.0)\times 10^{-11}$ s s^{-1} from RBS 1223 (Hambaryan et al. 2002) and $\sim 10^{-14}$ s s^{-1} from RX J0720.4-3125 (Zane et al. 2002) with inferred magnetic field strengths of $\sim 2 \times 10^{14}$ G and $\sim 10^{13}$ G, respectively, favour the models invoking a young (or middle-aged) cooling neutron star rather than the accretion heating, at least for these pulsating sources[1]. By virtue of this, the dim nearby neutron stars are suggested to be different from anomolous X-ray pulsars which have been proposed to be powered either by superstrong magnetic fields (Thompson & Duncan 1996) or accretion (Mereghetti & Stella 1995).

Following the spin history of the three known pulsars among the seven dim INSs and searching for pulsations in the others with new sensitive instruments is important for the understanding of the origin of their X-ray emission. Here we

Send offprint requests to: F. Haberl, e-mail: fwh@mpe.mpg.de

⋆ XMM-Newton is an ESA Science Mission with instruments and contributions directly funded by ESA Member states and the USA (NASA).

[1] Kaplan et al. (2002) derived a less stringent upper limit for $\dot{P}$ for RX J0720.4-3125 by not including XMM-Newton data, but also their results support the interpretation that this source is a cooling neutron star.

Table 1. XMM-Newton EPIC observations of RX J0806.4-4123 on November 8, 2000.

Camera	Read-out Mode	Filter	Observation Start	Observation End (UT)	Exp. [ks]
MOS1/2	FF, 2.6 s	Thin	13:43	18:47	18.0
pn	FF, 73 ms	Thin	14:24	18:53	15.6

report on an XMM-Newton observation of the poorly known INS RX J0806.4-4123. We present an improved X-ray position, the X-ray spectrum and the detection of a candidate for the rotation period of the star.

2. The XMM-Newton observation

XMM-Newton (Jansen et al. 2001) observed RX J0806.4-4123 during the satellite revolution #168 on November 8, 2000. Here we report on the analysis of the data collected with the European Photon Imaging Cameras (EPICs) based on MOS (EPIC-MOS1 and -MOS2, Turner et al. 2001) and pn (EPIC-pn, Strüder et al. 2001) CCD detectors which are mounted behind the three X-ray telescopes (Aschenbach et al. 2000). All cameras were operated in the Full-Frame mode (FF) providing data over a field of view of ∼13′ radius. Further details of the EPIC observations are summarized in Table 1. The data were processed using the XMM-Newton analysis package SAS version 5.2 to produce the photon event files and tools from version 5.3 for further spatial, spectral and timing analysis. The event times were corrected to solar barycenter using the SAS task "barycen 1.13.1" (in which a timing problem present in older versions has been solved).

2.1. The X-ray position of RX J0806.4-4123

Haberl et al. (1998) derived an error radius of 11″ (90% confidence) from the ROSAT PSPC observations of RX J0806.4-4123. The error is dominated by systematic uncertainties in the attitude reconstruction which could not be reduced due to the lack of other X-ray sources with optical counterparts detected in the field of view to define a reference coordinate frame. In order to find field stars in the EPIC images, a standard source detection analysis using combined box sliding and maximum likelihood techniques as available in SAS, was performed simultaneously in the three energy bands 0.3–1.0, 1.0–2.0 and 2.0–7.5 keV. This yielded 50, 29 and 33 detections with existence likelihood larger than 10 in the pn, MOS1 and MOS2 images, respectively. Figure 1 shows an EPIC-pn soft X-ray image. To identify possible optical counterparts to the X-ray sources, finding charts were produced using the DSS2 (red) image. To secure the identification, the following criteria were applied: (i) only X-ray sources which were detected by at least two EPIC instruments were used, (ii) a stellar-like object was found in the X-ray error circle, and (iii) both X-ray (spectral) and optical properties (R and B magnitudes as derived from the USNO A2.0 catalogue produced by the US Naval Observatory) must be compatible with a star. This resulted in the identification of five X-ray sources with field

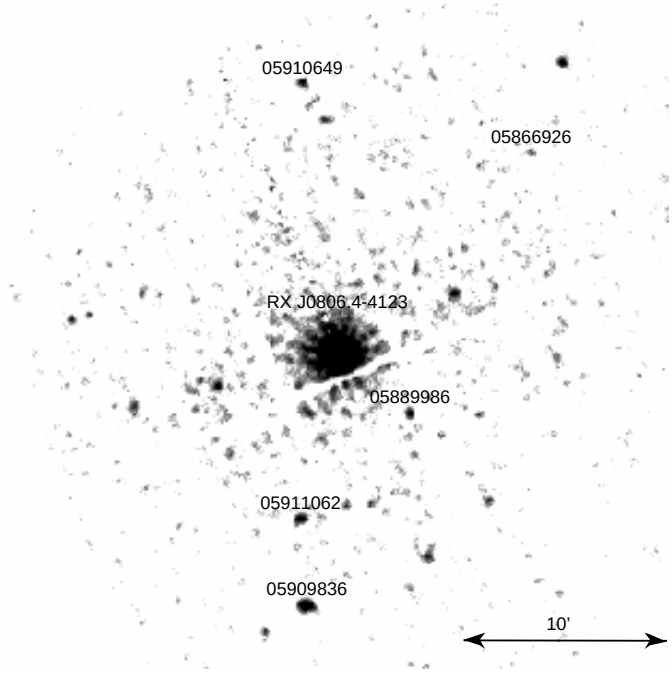

Fig. 1. EPIC-pn image in the 0.2–2.0 keV band. The image is smoothed with an adaptive intensity filter and out-of-time events (caused by photons detected during CCD-frame read-out) are subtracted on a statistical basis. Marked are the identified USNO A2.0 objects (see Table 2) used to define the coordinate reference frame.

stars as summarized in Table 2. Hardness ratios are defined as HR1 = $(B + A)/(B - A)$ and HR2 = $(C + B)/(C - B)$ with A, B and C as count rates in the energy bands 0.3–1.0, 1.0–2.0 and 2.0–7.5 keV, respectively. Coronal emission from stars is characterized by relatively soft X-ray spectra with the bulk of emission below 2 keV. This results in negative values for both hardness ratios with HR1 depending on the amount of interstellar absorption (see also Haberl 2002). HR2 values of weak sources are often undetermined due to the lack of statistics in the 2.0–7.5 keV band. For comparison the X-ray properties of the target are also shown in Table 2.

Using the SAS task "eposcorr" the X-ray source positions were corrected to the USNO A2.0 catalogue reference frame by minimizing the differences in X-ray to optical position for the five field stars. The uncertainties on the required coordinate shifts can be regarded as the remaining systematic error of the X-ray bore-sight and are 2.1″, 3.1″ and 2.5″ for pn, MOS1 and MOS2, respectively. Figure 2 shows the B-band image of the area around RX J0806.4-4123 as obtained by Haberl et al. (1998) with the three error circles derived from the EPIC instruments after the bore-sight correction. The corresponding position deduced from the pn image is RA = $08^{h}06^{m}23\overset{s}{.}47$ and Dec = –41°22′32″.3 (J2000.0). The error circles obtained from the EPIC data agree with each other and are completely inside the ROSAT circle. This confirms that none of the surrounding stars is responsible for the X-ray emission from RX J0806.4-4123.

Table 2. Field stars near RX J0806.4-4123 observed with EPIC pn.

ML[1]	count rate[2] [10^{-3} s^{-1}]	HR1	HR2	USNO counterpart	m_R [mag]	m_B [mag]
518	30.0 ± 2.5	−0.37 ± 0.08	−0.68 ± 0.15	U0450_05909836	13.0	14.0
124	8.5 ± 1.1	−0.22 ± 0.13	–	U0450_05911062	15.0	16.0
74	8.4 ± 1.4	−0.41 ± 0.15	−0.11 ± 0.32	U0450_05910649	15.3	16.5
46	3.7 ± 0.8	−0.61 ± 0.19	–	U0450_05889986	17.3	19.2
28	4.8 ± 1.2	−0.17 ± 0.26	–	U0450_05866926	13.3	14.5
10^5	1060 ± 10	−0.96 ± 0.01	−0.92 ± 0.06	–	–	–

[1] Likelihood for existence with probability $p_{\rm ML} = 1 - \exp(-{\rm ML})$.
[2] 0.3–2.0 keV.

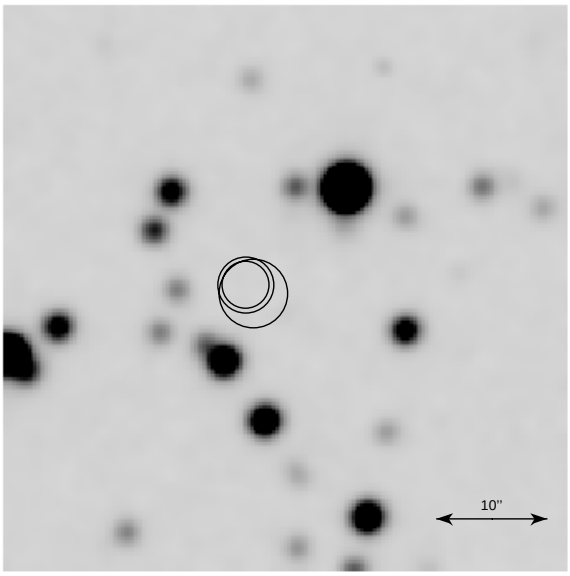

Fig. 2. *B*-band CCD image around the X-ray position of RX J0806.4-4123 (from Haberl et al. 1998). The circles represent the position uncertainties derived from pn (radius 2.1″), MOS1 (3.1″) and MOS2 (2.6″) which include statistical and (dominating) systematic X-ray errors and a 0.25″ error from the USNO A2.0 positions.

2.2. The temporal behaviour of RX J0806.4-4123

EPIC light curves of RX J0806.4-4123 were extracted in the 0.12–1.2 keV energy band (using events with pixel patterns 0–12) which covers most of the X-ray spectrum (see the next Section). The light curves show no significant variations over the duration of the observation with average net count rates of 1.81 cts s^{-1}, 0.369 cts s^{-1} and 0.405 cts s^{-1} in the pn, MOS1 and MOS2 detectors, respectively (Fig. 3). To search for periodicities on short time scales, we used 29 549 events extracted from a circle with radius of 45″ centered on the position of the target in the pn data. Of these selected events, about 97.5% were estimated to belong to the source. As a periodicity test we used the Rayleigh Z_n^2 method (Buccheri et al. 1983) with one harmonic involved ($n = 1$) which is expected to be optimal to search for rather smooth pulsations. The 0.073 s time resolution of the pn data limits the periodicity search to frequencies below ∼3 Hz. We performed the Z_1^2 test in the $\Delta f = 0.001$–3 Hz frequency range with a step of 5×10^{-6} Hz. The oversampling by a factor of 10 (compared to the expected widths of $1/T_{\rm sp}$ of the Z_1^2 peaks, where $T_{\rm sp} = 15.7$ ks is the observational time span) was chosen to resolve separate Z_1^2 peaks and to assure that no peak corresponding to a periodic signal is missing. As the variable Z_n^2 has a probability density function equal to that of χ^2 with $2 \cdot n$ degrees of freedom (e.g., Bendat & Piersol 1986), the probability to obtain a noise peak of a given Z_1^2 height in one trial is $\exp(-Z_1^2/2)$. The number of independent trials in the chosen frequency range estimated as $N = \Delta f\, T_{\rm sp} = 47.1 \times 10^3$ puts a lower limit on a Z_1^2 value to be yielded by a periodic signal with a probability $p > 0$, $Z_1^2 > 2\,\log(N) = 21.5$ (peaks with $Z_1^2 < 21.5$ are regarded as noise with a probability of 100%). This test resulted in only one peak higher than that lower limit, $Z_1^2 = 33.9$ at the frequency $f_* = 0.087936$ Hz (see Fig. 4). The probability to obtain by chance a peak of $Z_1^2 = 33.9$ in N independent trials is $p = N \exp(-Z_1^2/2) = 2.0 \times 10^{-3}$, which corresponds to a detection of pulsations at a confidence level of $C = (1 - p) \times 100\% = 99.8\%$, or 3.1σ. Involving higher harmonics gives values $Z_2^2 = 42.9$, $Z_3^2 = 43.0$ and $Z_4^2 = 43.2$ at the same frequency f_*. These numbers indicate that, according to the H-test suggested by de Jager et al. (1989), there is a statistically significant contribution from the second harmonic. A probability to obtain a noise peak of $Z_2^2 = 42.9$ in one trial is only $p = 1.1 \times 10^{-8}$ and in N independent trials is $p = 5.1 \times 10^{-4}$, that increases the significance of the period detection up to a 3.5σ level. We note this Z_2^2 peak is highest in the frequency range chosen for the periodicity search (all other Z_2^2 peaks are below 27.0 and produced by noise with probabilities $p > 94\%$). We also performed the Z_n^2-test adding 14 210 source photons detected with two MOS cameras to the pn data. The increase of the total statistics by about 50% results only in small increments in Z_n^2 values ($Z_1^2 = 37.5$ and $Z_2^2 = 43.9$ at the same frequency f_*) and significance of the detected signal (to a 3.6σ level). That can be explaind by the low time resolution of the MOS data (see Table 1) which should lead to a strong smearing of the weak signal.

To determine the pulsation frequency and its uncertainties more accurately, we applied the Odds-ratio method by Gregory & Loredo (1996) based on the Bayesian formalism. The frequency-dependent Odds-ratio $O(f)$ specifies how the data favour a periodic model of a frequency f over the

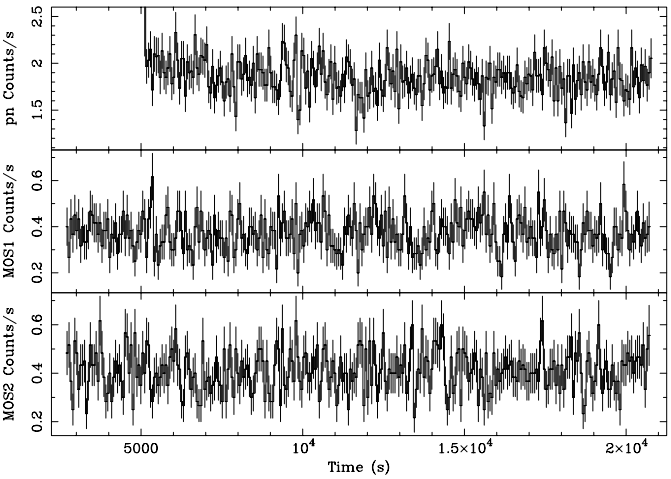

Fig. 3. EPIC light curves with a time resolution of 60 s derived from the 0.12–1.2 keV energy band. The background with average values of 3.9×10^{-2} cts s^{-1}, 3.1×10^{-3} cts s^{-1} and 4.5×10^{-3} cts s^{-1} for pn, MOS1 and MOS2, respectively, is not subtracted. Start time is 2000, Nov. 8, 13:45:12 UT.

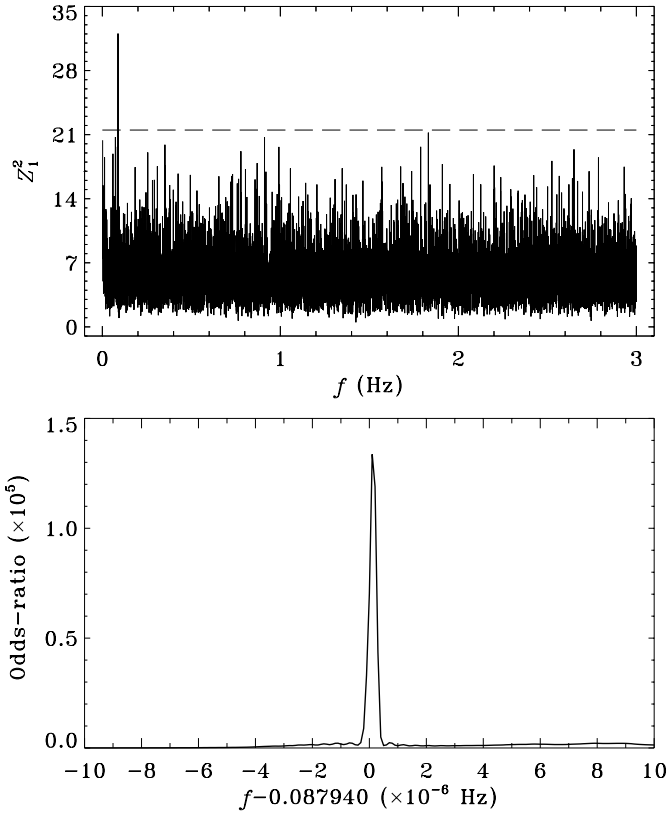

Fig. 4. Power spectrum (top panel) and frequency dependence of the Odds-ratio. The dashed line in the top panel shows a $Z_1^2 = 21.5$ level below which all peaks can be regarded as noise with a probability of 100%.

unpulsed model. This ratio allows one to obtain the probability distribution function $p(f) \propto O(f)f^{-1}$ for a signal to be periodic in a chosen frequency range (see Zavlin et al. 2000, for more details). Figure 4 shows the dependence of $O(f)$ in a range around the frequency f_* resulting from the Z_1^2 test. The maximum value $O_{\max} = 1.3 \times 10^5$ is at $f = f_0 = 0.087940$ Hz ($f_0 - f_* = 4 \times 10^{-7}$ Hz $\ll 1/T_{\rm sp}$). The uncertainties of f_0 at the 68% and 90% confidence levels are $\delta f = 2.3 \times 10^{-6}$ and 10.5×10^{-6} Hz, respectively. The corresponding rotation period is $P_0 = 11.37139$ s with uncertainties of 3.0×10^{-4} and 13.6×10^{-4} s at the 68% and 90% levels, respectively.

The folded light curve extracted at $f = f_0$ from the pn data (see Fig. 5) reveals one broad pulse per period with the pulsed fraction of $f_{\rm p} = 6.2 \pm 1.0\%$. The MOS light curve extracted at $f = f_0$ shows a remarkable similarity with that obtained from the pn data (Fig. 5), although the MOS time resolution makes its pulse somewhat broader and pulsed fraction smaller than those in the pn light curve. We also note that the ROSAT PSPC observation of RX J0806.4-4123 in October 1993 yielded too scanty statistics (about 900 counts) for searching a signal of such a small pulsed fraction (the signal should result in a too low peak with $Z_1^2 \sim 1$, which cannot be discriminated from the noise).

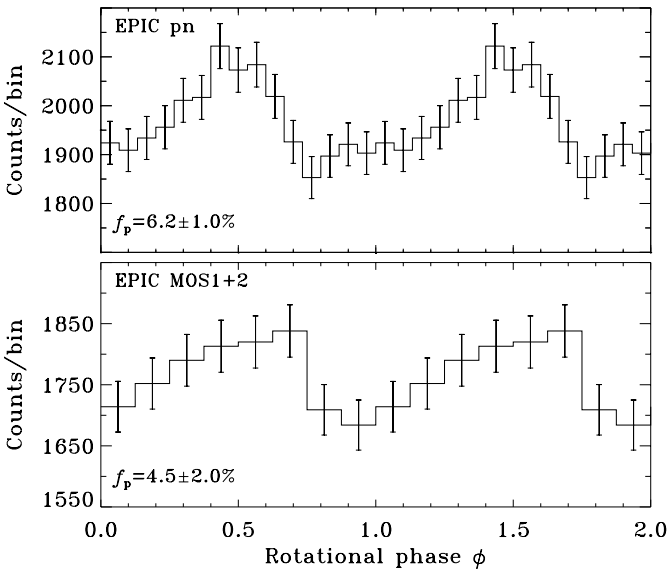

Fig. 5. Pulse profiles extracted from the pn (top panel) and combined MOS1 and MOS2 data from RX J0806.4-4123 at $f = f_0 = 0.087940$ Hz.

2.3. The X-ray spectrum of RX J0806.4-4123

The X-ray spectra were extracted using single- and double-pixel events (pattern 0–4) from pn and pattern 0–12 events from MOS data. Detector response matrix files were used as available from the hardware groups in November 2001 (version 6.1 for pn and v9q20t5r6 for MOS). First, an absorbed blackbody model with normalization parameters allowed to be free for the individual instruments was simultaneously fitted to the three spectra (left panels in Fig. 6). From the best fit a blackbody temperature of $kT^\infty = 94 \pm 1$ eV[2] and an upper limit for the hydrogen column density $n_{\rm H}$ of 10^{18} cm^{-2} were found

[2] The superscript $^\infty$ is used to indicate that quantities are given as measured by a distant observer. Errors on the spectral parameters are given at a 90% confidence level.

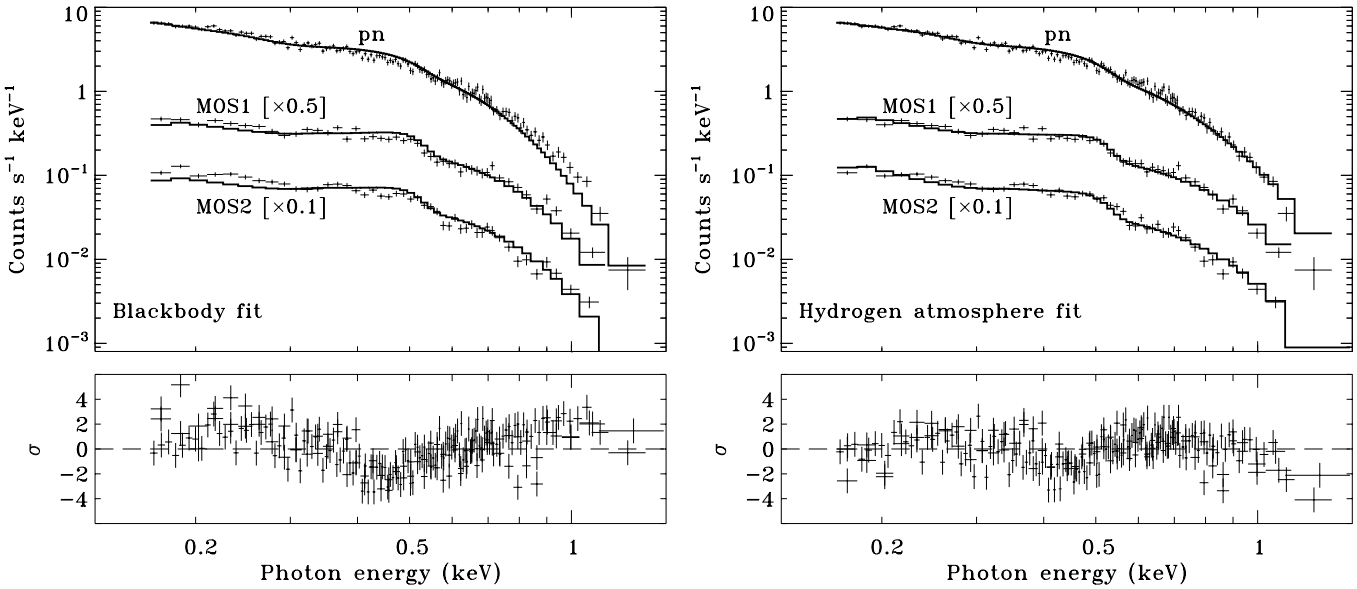

Fig. 6. EPIC spectra of RX J0806.4-4123 together with the best fit blackbody (left) and atmosphere (right) models. Most of the residuals (shown in the bottom panels) are probably caused by calibration uncertainties around instrumental absorption edges.

(χ^2_ν = 2.9 for 228 degrees of freedom, dof). The low value for the absorption may be caused by calibration uncertainties mainly below 0.5 keV. The radius of the emitting area derived from the blackbody fit is $R^\infty \simeq 0.6\,(d/100\,\mathrm{pc})$ km. Fitting the pn and MOS spectra separately yields blackbody temperatures of kT^∞ = 97 ± 1 eV and 91 ± 1 eV for the pn and MOS data, respectively (χ^2_ν = 2.5 for 224 dof). The model fluxes in the 0.1–2.4 keV range, 2.82×10^{-12} erg cm^{-2} s^{-1}, 3.08×10^{-12} erg cm^{-2} s^{-1} and 3.38×10^{-12} erg cm^{-2} s^{-1} as derived from the combined fit for the pn, MOS1 and MOS2 spectra (respectively), show differences between the three instruments larger than the typical statistical errors of 1–2% obtained from the fit. For comparison, Haberl et al. (1998) derived a flux of $(2.9^{+0.30}_{-0.15})\times10^{-12}$ erg cm^{-2} s^{-1} (90% confidence) from the ROSAT PSPC data.

Nonmagnetic neutron star hydrogen atmosphere models (Zavlin et al. 1996)[3] fit the pn and MOS spectra fairly well, resulting in the surface temperature $kT^\infty \simeq 26$ eV and a 110 pc distance to RX J0806.4-4123 assuming the "canonical" neutron star radius $R_{\rm NS}$ = 10 km and mass $M_{\rm NS} = 1.4\,M_\odot$ (χ^2_ν = 1.8 for 228 d.o.f.; right panels in Fig. 6). To account for systematic calibration uncertainties, $n_{\rm H}$ was allowed to vary in fits to the spectra from the different instruments, while the surface temperature and distance were kept at the same values for all three spectra. The obtained values of the hydrogen column density are $n_{\rm H} \simeq 1.6\times10^{20}$ cm^{-2}, 1.0×10^{20} cm^{-2} and 0.4×10^{20} cm^{-2} for the fits to the pn, MOS1 and MOS2 data, respectively. Neither pure iron nor solar-mixture atmosphere models fit the EPIC spectra of RX J0806.4-4123 ($\chi^2_\nu \simeq 20$).

[3] The hydrogen atmosphere models are available at `http://legacy.gsfc.nasa.gov/docs/xanadu/xspec`

3. Discussion

The XMM-Newton observations of the INS candidate RX J0806.4-4123 revealed pulsations in its X-ray flux with a period of 11.3714 s. This is well within the range of 5.16 s to 22.7 s observed from three other dim INSs. Although detected at a statistical level of 3.5σ, the similar pulse profiles seen in the data from all EPIC instruments inspire confidence that the modulation is real and indicates the rotation period of the neutron star. The pulsed fraction of 6.2% is the weakest detected so far in X-rays from these objects (9% in the X-ray flux of RX J0720.4-3125, Cropper et al. 2001; 20 ± 2% in RBS 1223, Hambaryan et al. 2002; 43 ± 14% in RX J0420.0-5022, Haberl et al. 1999). Such a modulation is too small to be found in available data of any of the other dim INSs. For example, only an upper limit of 4.5% was derived from a 450 ks Chandra observation of RX J1856.5-3754 (Ransom et al. 2002). A simplest explanation for a small pulsed fraction in X-ray radiation from an INS is that the rotational axis of the star is nearly co-aligned with either the line of sight to a distant observer or the magnetic axis of the star (or both). Another reason resulting in the small pulsed fraction can be the effect of light bending in the strong gravitational field near the neutron star surface (e.g. Pechenick et al. 1983; Riffert & Mészáros 1988), For instance, if a neutron star is rather massive, so that $[M_{\rm NS}/M_\odot]/[R_{\rm NS}/1\ \mathrm{km}] > 0.177$, the whole star's surface becomes visible (e.g. Zavlin et al. 1995b), which should result in a strong smearing of the modulated X-ray flux emitted by the neutron star (even if the radiation originates from a small spot on the star's surface). However, assuming that radii and masses of the detected INSs are clustering around the canonical values of $R_{\rm NS}$ = 10 km and $M_{\rm NS} = 1.4\,M_\odot$, we may conclude that the different observed pulsed fractions are mainly caused by geometrical effects, namely, different orientations of the stars' axes and/or different sizes of the emitting areas.

In this respect it is interesting that for the two dim INSs with the estimates on strength of the surface magnetic fields, $\sim 2 \times 10^{13}$ G for RX J0720.4-3125 (Zane et al. 2002) and $\sim 2 \times 10^{14}$ G for RBS 1223 (Hambaryan et al. 2002), the pulsed fraction in the X-ray flux from the object with the stronger field is significantly higher, as is expected if the radiation is emitted from hot spots around the magnetic poles. Hot polar caps can either be produced by a flux of relativistic particles falling down onto the polar caps from the pulsar magnetosphere or anisotropy of the thermal conductivity in the neutron star crust caused by a very strong magnetic field (see, e.g., Greenstein & Hartke 1983). While it looks feasible to explain the shallow modulation observed from RX J0806.4-4123 by the anisotropic heat conduction, Cropper et al. (2001) argue that the relatively smooth temperature gradient on the neutron star surface produced by this mechanism alone can only marginally explain the pulse profile of RX J0720.4-3125. Higher pulsed fractions will be even more difficult to reconcile with this model, unless the surface radiation is intrinsically anisotropic as it may emerge from a magnetized neutron star atmosphere (Pavlov et al. 1994; Zavlin et al. 1995a). It is clear that whatever mechanism produces the hot polar regions, measuring rotational period changes and, therefore, magnetic field strengths for the pulsating dim INS is crucial for understanding the origin of their X-ray emission.

The EPIC spectral data on RX J0806.4-4123 are well consistent with a smooth, featureless model and can be fitted with both blackbody and neutron star hydrogen (or helium) atmosphere spectra (since there are still fairly large uncertainties in the calibration of the instrument responses at energies below 0.5–0.6 keV, we do not consider the blackbody approach as rejected by the data because of the rather poor quality of the spectral fit). The derived blackbody temperature of $\simeq$94 eV is within the range of values found for other X-ray dim neutron stars, in particular, it is close to that of RX J1605.3+3249 (Motch et al. 1999). Extrapolating the best-fit blackbody model to the optical wavelength range gives a B magnitude $m_B \simeq 30.8$ (neglecting extinction) for a possible optical counterpart – much fainter flux than the upper limit put by Haberl et al. (1998). It is worthwhile to mention that the optical counterparts found for the INSs RX J1856.5-3754 and RX J0720.4-3125 are significantly brighter than the extrapolations of the blackbody spectra obtained from the X-ray data on these two objects (Pons et al. 2002; Motch & Haberl 1998). The hydrogen atmosphere model fit predicts $m_B \simeq 26.9$, still in agreement with the upper limit $m_B > 24$. On the other hand, optical fluxes predicted by the light-element atmosphere models for RX J1856.5-3754 (Pavlov et al. 1996; Pons et al. 2002) and RX J0720.4-3125 (Motch & Haberl 2002) are much brighter than the actually measured values. If RX J0806.4-4123 has properties similar to those of these two INSs, then the B magnitude of its optical flux is expected to be in the range of 28–30. Utilizing the improved X-ray position derived from the XMM-Newton data on RX J0806.4-4123, more stringent constraints on the neutron star parameters can be obtained from future deep optical observations.

Acknowledgements. The XMM-Newton project is supported by the Bundesministerium für Bildung und Forschung / Deutsches Zentrum für Luft- und Raumfahrt (BMBF / DLR), the Max-Planck-Gesellschaft and the Heidenhain-Stiftung.

References

Aschenbach, B., Briel, U. G., Haberl, F., et al. 2000, in X-Ray Optics, Instruments, and Missions III, ed. Joachim E. Trümper, & B. Aschenbach, SPIE Proc., 4012, 731
Bendat, J. S., & Piersol, A. G. 1986, in Random Data: Analysis and Measurement Procedures (Wiley: New York)
Buccheri, R., Bennett, K., Bignami, et al. 1983, A&A, 128, 245
Burwitz, V., Zavlin, V. E., Neuhäuser, R., et al. 2001, A&A, 379, L35
Cropper, M., Zane, S., Ramsay, G., Haberl, F., & Motch, C. 2001, A&A, 365, L302
de Jager, O. C., Raubenheimer, B. C., & Swanepoel, J. W. H. 1989, A&A, 221, 180
Greenstein, G., & Hartke, G. J. 1983, ApJ, 271, 283
Gregory, P. C., & Loredo, T. J. 1996, ApJ, 473, 1059
Haberl, F. 2002, in New Visions of the X-ray Universe in the XMM-Newton and Chandra Era, ESA SP-488, in press
Haberl, F., Motch, C., Buckley, D. A. H., Zickgraf, F. J., & Pietsch, W. 1997, A&A, 326, 662
Haberl, F., Motch, C., & Pietsch, W. 1998, Astronomische Nachrichten, 319, 97
Haberl, F., Pietsch, W., & Motch, C. 1999, A&A, 351, L53
Hambaryan, V., Hasinger, G., Schwope, A. D., & Schulz, N. S. 2002, A&A, 381, 98
Jansen, F., Lumb, D., Altieri, B., et al. 2001, A&A, 365, L1
Kaplan, D. L., Kulkarni, S. R., van Kerkwijk, M. H., & Marshall, H. L. 2002, ApJ, 570, L79
Kulkarni, S. R., & van Kerkwijk, M. H. 1998, ApJ, 507, L49
Mereghetti, S., & Stella, L. 1995, ApJ, 442, L17
Motch, C. 1999, in X-ray Astronomy, Stellar Endpoints, AGN, and the Diffuse X-ray Background, AIP Conf. Proc., 599, 244
Motch, C., & Haberl, F. 1998, A&A, 333, L59
Motch, C., & Haberl, F. 2002, in preparation
Motch, C., Haberl, F., Zickgraf, F. J., Hasinger, G., & Schwope, A. D. 1999, A&A, 351, 177
Paerels, F., Mori, K., Motch, C., et al. 2001, A&A, 365, L298
Pavlov, G. G., Shibanov, Y. A., Ventura, J., & Zavlin, V. E. 1994, A&A, 289, 837
Pavlov, G. G., Zavlin, V. E., Trümper, J., & Neuhäuser, R. 1996, ApJ, 472, L33
Pechenick, K. R., Ftaclas, C., & Cohen, J. M. 1983, ApJ, 274, 846
Pons, J. A., Walter, F. M., Lattimer, J. M., et al. 2002, ApJ, 564, 981
Ransom, S. M., Gaensler, B. M., & Slane, P. O. 2002, ApJ, 570, L75
Riffert, H., & Mészáros, P. 1988, ApJ, 325, 207
Strüder, L., Briel, U., Dennerl, K., et al. 2001, A&A, 365, L18
Thompson, C., & Duncan, R. C. 1996, ApJ, 473, 322
Treves, A., Turolla, R., Zane, S., & Colpi, M. 2000, PASP, 112, 297
Turner, M. J. L., Abbey, A., Arnaud, M., et al. 2001, A&A, 365, L27
Walter, F. M., & Matthews, L. D. 1997, Nature, 389, 358
Walter, F. M., Wolk, S. J., & Neuhäuser, R. 1996, Nature, 379, 233
Zampieri, L., Campana, S., Turolla, R., et al. 2001, A&A, 378, L5
Zane, S., Haberl, F., Cropper, M., et al. 2002, MNRAS, in press
Zavlin, V. E., Pavlov, G. G., Sanwal, D., & Trümper, J. 2000, ApJ, 540, L25
Zavlin, V. E., Pavlov, G. G., & Shibanov, Y. A. 1996, A&A, 315, 141
Zavlin, V. E., Pavlov, G. G., Shibanov, Y. A., & Ventura, J. 1995a, A&A, 297, 441
Zavlin, V. E., Shibanov, Y. A., & Pavlov, G. G. 1995b, Astron. Lett., 21, 168